



HAL
open science

Electronic structures and magnetic performance related to spintronics of Sr_{0.875}Ti_{0.125}S

Ali Bourega, Bendouma Doumi, Allel Mokaddem, Adlane Sayede, Abdelkader
Tadjer

► **To cite this version:**

Ali Bourega, Bendouma Doumi, Allel Mokaddem, Adlane Sayede, Abdelkader Tadjer. Electronic structures and magnetic performance related to spintronics of Sr_{0.875}Ti_{0.125}S. *Optical and Quantum Electronics*, 2019, 51 (12), 10.1007/s11082-019-2107-2 . hal-02449162

HAL Id: hal-02449162

<https://hal.science/hal-02449162>

Submitted on 27 Nov 2023

HAL is a multi-disciplinary open access archive for the deposit and dissemination of scientific research documents, whether they are published or not. The documents may come from teaching and research institutions in France or abroad, or from public or private research centers.

L'archive ouverte pluridisciplinaire **HAL**, est destinée au dépôt et à la diffusion de documents scientifiques de niveau recherche, publiés ou non, émanant des établissements d'enseignement et de recherche français ou étrangers, des laboratoires publics ou privés.

Electronic structures and magnetic performance related to spintronics of $\text{Sr}_{0.875}\text{Ti}_{0.125}\text{S}$

Ali Bourega¹ · Bendouma Doumi^{2,3} · Allel Mokaddem^{3,4} · Adlane Sayede⁵ · Abdelkader Tadjer⁶

Abstract

In this study, we have used the first-principle approaches of density functional theory to determine the electronic and magnetic performances related to spintronics applications of titanium (Ti)-substituted SrS such as $\text{Sr}_{1-x}\text{Ti}_x\text{S}$ at concentration $x = 0.125$. The results of electronic and magnetic properties by using TB-mBJ potential revealed that $\text{Sr}_{0.875}\text{Ti}_{0.125}\text{S}$ compound is half-metallic ferromagnetic with a half-metallic gap and a spin polarization of 100%. The ferromagnetic nature of $\text{Sr}_{0.875}\text{Ti}_{0.125}\text{S}$ material is confirmed by the ferromagnetic coupling between magnetic moments of Ti, Sr and S atoms. The total magnetic moment of integer Bohr magneton of $2 \mu_B$ and the large half-metallic gap of 1.245 suggest that this compound is a true half-metallic ferromagnet.

Keywords Electronic structures · Half-metallic ferromagnetism · Ti-substituted SrS · TB-mBJ

✉ Bendouma Doumi
bdoummi@yahoo.fr; bdoumma@gmail.com

✉ Allel Mokaddem
mokaddem.allel@gmail.com

¹ Laboratory of Physico-Chemical Studies, Dr. Tahar Moulay University of Saida, 20000 Saida, Algeria

² Department of Physics, Faculty of Sciences, Dr. Tahar Moulay University of Saida, 20000 Saida, Algeria

³ Laboratoire d'Instrumentation et Matériaux Avancés, Centre Universitaire Nour Bachir El Bayadh, BP 900 route Aflou, 32000 El Bayadh, Algeria

⁴ Centre Universitaire Nour Bachir El Bayadh, 32000 El Bayadh, Algeria

⁵ Unité de Catalyse et Chimie du Solide (UCCS), UMR CNRS 8181, Faculté des Sciences, Université d'Artois, Rue Jean Souvraz, SP 18, 62307 Lens, France

⁶ Modelling and Simulation in Materials Science Laboratory, Physics Department, Djillali Liabes University of Sidi Bel-Abbes, 22000 Sidi Bel-Abbes, Algeria

1 Introduction

The diluted magnetic semiconductors (DMS) have been the subject of several experimental and theoretical studies to improve the performance of their properties for magneto-electronics applications (Cui et al. 2019; Berriah et al. 2018; Lakhdari et al. 2019; Yunusov et al. 2018; Torquato et al. 2018; Miyagawa et al. 2019; Emam-Ismail et al. 2019). These compounds are potential candidates for modern spintronics due to their magnetic and semiconductor characters, which can be generated by the doping magnetic transitions or rare earths ions in the host semiconductors. In the spintronics devices, the spin (magnetic moment) of the electron in addition to its charge is explored as another degree of freedom. However, the DMS are used in logic function gates and storage devices due to these particular features (Ghosh et al. 2019b). It is necessary to understand the importance of high Curie temperature (TC) of half-metallic materials for spintronics (Lei et al. 2016). The wide-band gap semiconductors based half-metallic DMS are suitable materials for applications of spintronics devices because they show the stability of the ferromagnetism at temperatures higher than the room temperature (Sato and Katayama-Yoshida 2001; Wu et al. 2003). Dietl et al. (2000) have predicted high-TC ferromagnetism in the GaN doped Mn, using a mean field approximation of Zener carrier-mediated model. Recently, Wang et al. (2014) have obtained an accurate TC of 178 ± 1 K for (Ga, Mn)As DMS using experimental simultaneous magnetometry and transport measurements. Although, the high TC can be estimated in the half-metallic materials with wide half-metallic gaps (Saini et al. 2012).

The SrS is one of the II–VI strontium chalcogenides such as SrX (X = S, Se and Te), they shape closed-shell ionic compounds crystallized in rock-salt NaCl (B1) structure under ambient conditions (Dadsetani and Pourghazi 2006; Bhattacharjee and Chattopadhyaya 2017a; Debnath et al. 2018). These materials are important semiconductors owing to their large band gaps and valence-band widths with significant technological applications in the field of microelectronics, catalysis, radiation dosimetry, luminescent and infrared sensitive devices, and fast high resolution optically stimulated luminescence imaging (Ruoff and Grzybowski 1985; Pandey and Sivaraman 1991; Yamashita et al. 1984; Varshney et al. 2008).

Recently, the electronic structures and magnetism in the II–VI semiconductors based DMS have been extensively studied experimentally and theoretically (Berriah et al. 2018; Yang et al. 2016; Addadi et al. 2017; Linneweber et al. 2017; Shahjahan and Nizu 2018; Salam 2019; Ghosh et al. 2019a). Among these materials, the SrX strontium chalcogenides are considered as potential DMS candidates according to the theoretical predictions of electronic structures, half-metallic behavior and the existence of ferromagnetism in vanadium (V)- and chromium (Cr)-substituted SrS, SrSe and SrTe (Doumi et al. 2015a,d). Recently, Lin et al. (2017) have used first-principle calculations to predict that the hole doping can induce ferromagnetism in SrS and SrSe monolayer sheets.

The objective of this study is to investigate the structural, electronic and half-metallic ferromagnetic properties of Ti-substituted SrS such as $\text{Sr}_{1-x}\text{Ti}_x\text{S}$ compound at concentration $x=0.125$. We have used in our calculations the generalized gradient approximation functional (GGA–WC) (Wu and Cohen 2006) and the Tran–Blaha modified Becke–Johnson (TB–mBJ) potential (Tran and Blaha 2009; Becke and Johnson 2006) based on full-potential linearized augmented plane-wave method within first-principle approaches of density functional theory (Hohenberg and Kohn 1964; Kohn and Sham 1965).

2 Method and details of calculations

The SrS belongs to the II–VI strontium chalcogenides, crystallizing in the rock-salt NaCl (B1) phase. The conventional structure of SrS has space group of ($Fm\bar{3}m$) No. 225, which Sr and S atoms are situated at the (0, 0, 0) and (0.5, 0.5, 0.5) sites, respectively. The $Sr_{1-x}Ti_xS$ ($1 \times 1 \times 2$) supercell of 16 atoms with concentration $x=0.125$ is created by substituting of Sr atom by the Ti impurity at (0, 0, 0) position. We have obtained the tetragonal structure of $Sr_{0.875}Ti_{0.125}S$ with space group of ($P4/mmm$) No. 123. The supercell of $Sr_{0.875}Ti_{0.125}S$ is described by a structure closed to the stoichiometric ordered structure in order to avoid side effects as defects on this ordered structure. We have employed the full-potential linearized augmented plane-wave (FP-LAPW) method based on density functional theory (DFT) (Hohenberg and Kohn 1964; Kohn and Sham 1965) as implemented in the WIEN2 K package (Blaha et al. 2001) to determine the structural, electronic and half-metallic ferromagnetic properties of $Sr_{0.875}Ti_{0.125}S$. The augmented plane wave (APW) method supposes that the crystalline potential is replaced by its spherical average in the Muffin-tin spheres and it is constant in the interstitial zone between the spheres. However, the full-potential FP-LAPW improves the APW method, which provides continuity of potential at the surfaces of Muffin-tin spheres (Singh and Nordstrom 2006).

The structural properties are calculated by using of the generalized gradient approximation functional (GGA–WC) (Wu and Cohen 2006), whereas the electronic structures and magnetic moments are calculated with Tran–Blaha modified Becke–Johnson (TB–mBJ) exchange potential combined with local density correlation potential (Tran and Blaha 2009; Becke and Johnson 2006). The average radii of Muffin-tin spheres of the Sr, S and Ti atoms have been taken in condition that the spheres do not overlap. The cutoff of -6 Ry is employed to describe the separation between the valence and the core states. In the interstitial site of crystal, the wave functions have expanded to plane waves by means of a cut-off $K_{max} = 9.0/R_{MT}$. The K_{max} defines the average radius of the muffin–tin sphere and the K_{max} represents the size of the largest K vector in the plane wave. We have performed the Brillouin-zone sampling by the use of the Monkhorst–Pack mesh (Monkhorst and Pack 1976; Pack and Monkhorst 1977) of ($4 \times 4 \times 4$) k-points for SrS and ($4 \times 4 \times 2$) k-points for $Sr_{0.875}Ti_{0.125}S$. The Self-consistent was obtained when the total energy converges towards 0.1 mRy.

3 Results and discussions

3.1 Structural properties

We have employed the empirical Murnaghan equation of state (Murnaghan 1944) to adjust the curves of the total energies as a function of the volumes in order to calculate the structural parameters. The results of the lattice constants (a), bulk modulus (B) and their pressure derivatives (B') for the SrS and the $Sr_{0.875}Ti_{0.125}S$ with other experimental (Syassen 1985) and theoretical (Bhattacharjee and Chattopadhyaya 2017a; Debnath et al. 2018) data are given in Table 1. The structural parameters a and B of binary SrS have good concordance with the experimental data (Syassen 1985) and they are close to the theoretical calculations (Bhattacharjee and Chattopadhyaya 2017a; Debnath et al. 2018) found by the same GGA–WC potential. This is due to the better performance of the GGA–WC for calculating

Table 1 Computed lattice constants (a), bulk modules (B) and their pressure derivatives (B') for SrS and Sr_{0.875}Ti_{0.125}S compounds

Compound	a (Å)	B (GPa)	B'	Method
This work				
SrS	5.973	52.90	4.36	GGA–WC
Sr _{0.875} Ti _{0.125} S	5.873	55.78	4.32	GGA–WC
Other calculations				
SrS	5.976 ^a	52.54 ^a	4.335 ^a	GGA–WC
	5.976 ^b	53.049 ^b	4.734 ^b	GGA–WC
	6.024 ^c	58.0 ^c		Experimental

^aBhattacharjee and Chattopadhyaya (2017a)

^bDebnath et al. (2018)

^cSyassen (1985)

structural properties of solids (Wu and Cohen 2006; Doumi et al. 2015b, c; Sajjad et al. 2015). The lattice constant of Sr_{0.875}Ti_{0.125}S decreased due to the difference between the Ti and Sr ionic radii, meaning that the Sr_{0.875}Ti_{0.125}S is harder compared to the SrS. We haven't found any experimental and theoretical studies on the Sr_{0.875}Ti_{0.125}S in order to compare them with our results.

3.2 Electronic structures and half-metallic behavior

The electronic structures are performed by the use of TB–mBJ semi-local exchange–correlation potential due to its performance for calculating band structures (Tran and Blaha 2009; Becke and Johnson 2006). The plots of band structures at the high symmetry points

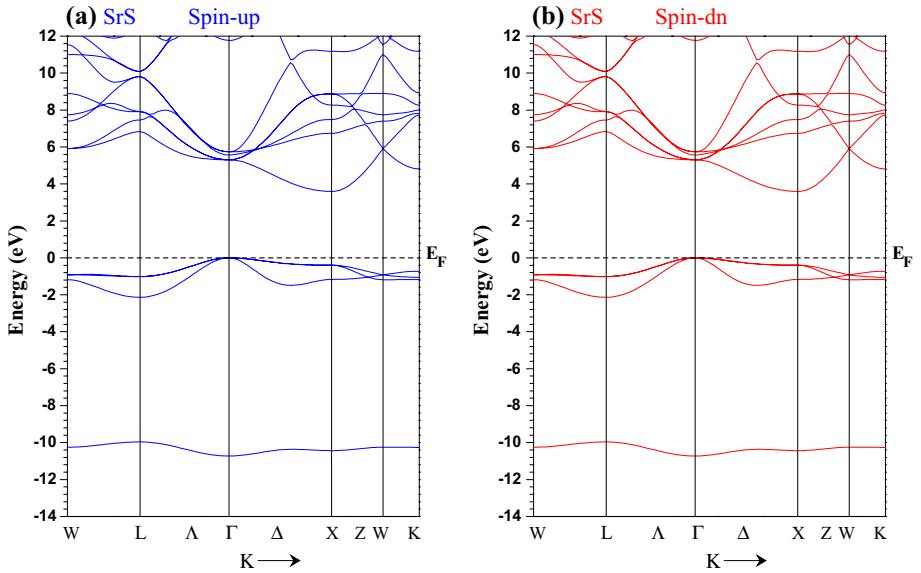


Fig. 1 Spin-polarized band structures for SrS. **a** Majority spins (up) and **b** Minority spins (dn). (Fermi level (E_F) is set to zero)

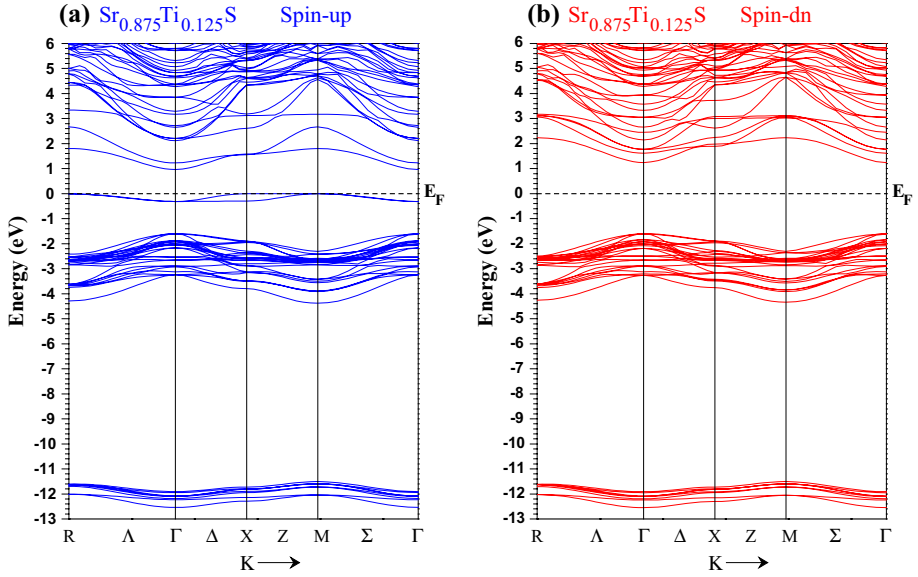


Fig. 2 Spin-polarized band structures for $\text{Sr}_{0.875}\text{Ti}_{0.125}\text{S}$. **a** Majority spins (up) and **b** Minority spins (dn). (Fermi level (E_F) is set to zero)

of Brillouin-zone of SrS and $\text{Sr}_{0.875}\text{Ti}_{0.125}\text{S}$ compounds are displayed by the Figs. 1 and 2, respectively. The compound $\text{Sr}_{0.875}\text{Ti}_{0.125}\text{S}$ is created from the substituting Ti atom in the supercell of 8 atoms of SrS wide-gap semiconductor. The magnetic Ti atom is placed at Sr cationic site in such a way that the magnetic spins of the 3d-Ti states are injected into SrS, which influence the electronic structures and induce the magnetism in the $\text{Sr}_{0.875}\text{Ti}_{0.125}\text{S}$ compound. As result, the majority spins become metallic owing to localized electrons of 3d-Ti majority-spin states in the gap, while the minority spins keep semiconductor behavior of SrS because the 3d-Ti empty minority-spin states are located into bottom of conduction band far than Fermi level. Consequently, the $\text{Sr}_{0.875}\text{Ti}_{0.125}\text{S}$ compound becomes half-metallic ferromagnetic with spin polarization of 100%.

The Fig. 1 shows similar band structures for two spins directions of SrS. The SrS depicts an indirect band gap ($E^{\Gamma X}$), which occurs between the valence band maximum (VBM) and the conduction band minimum (CBM) situated at Γ and X high symmetry points, respectively. The majority-spin bands of $\text{Sr}_{0.875}\text{Ti}_{0.125}\text{S}$ compound are metallic due to localized partially filled 3d-Ti majority-spin levels in the gap around Fermi level (E_F). For the minority-spin bands of $\text{Sr}_{0.875}\text{Ti}_{0.125}\text{S}$, the valence band minimum is located at the Γ high symmetry point like SrS, whereas the conduction band minimum occurs at Γ high symmetry, which is formed by the 3d-Ti empty anti-bonding states far than E_F , generating a direct band gap at Γ high symmetry. Consequently, the SrS shifts from indirect band gap ΓX to direct band gap $\Gamma \Gamma$ for $\text{Sr}_{0.875}\text{Ti}_{0.125}\text{S}$.

The $\text{Sr}_{0.875}\text{Ti}_{0.125}\text{S}$ compound has a gap for minority spin, while its majority spin exhibits metallic feature (see Fig. 2). The minority-spin bands of $\text{Sr}_{0.875}\text{Ti}_{0.125}\text{S}$ are characterized by two important factors; the half-metallic ferromagnetic (HMF) gap (G_{HMF}) and the half-metallic (HM) gap (G_{HM}). The first determines the fundamental band gap, whereas the second defines the minimal energy band gap for a spin-flip of minority spin (Doumi et al. 2015a, d; Cherfi et al. 2016). The HMF and HM gaps features have been observed

in the V- and Cr-doped SrS materials such as $\text{Sr}_{0.875}\text{V}_{0.125}\text{S}$ (Doumi et al. 2015a) and $\text{Sr}_{0.875}\text{Cr}_{0.125}\text{S}$ (Doumi et al. 2015d). The half-metal gaps are 0.937 and 0.815 eV respectively for $\text{Sr}_{0.875}\text{V}_{0.125}\text{S}$ and $\text{Sr}_{0.875}\text{Cr}_{0.125}\text{S}$, which are located between the valence band maximum and Fermi level (E_F). In distinguish, the d-Ti anti-bonding states of minority spin shift towards low energies, moving the conduction band minimum towards E_F and valence band minimum far than E_F . Therefore, the half-metal gap of $\text{Sr}_{0.875}\text{Ti}_{0.125}\text{S}$ changes its position with respect to E_F , which occurs between E_F and the conduction band minimum. In this case, the half-metal gap of 1.245 eV for $\text{Sr}_{0.875}\text{Ti}_{0.125}\text{S}$ is better than that of $\text{Sr}_{0.875}\text{V}_{0.125}\text{S}$ and $\text{Sr}_{0.875}\text{Cr}_{0.125}\text{S}$. The wide HM gap makes the $\text{Sr}_{0.875}\text{Ti}_{0.125}\text{S}$ compound potential candidate for spin-injection applications in semiconductor spintronics.

Table 2 summarizes the results of indirect gap ($E^{\Gamma X}$) of SrS, and the G_{HMF} and G_{HM} of $\text{Sr}_{0.875}\text{Ti}_{0.125}\text{S}$ with other theoretical (Bhattacharjee and Chattopadhyaya 2017a, b; Debnath et al. 2018) and experimental (Kaneko and Koda 1988) values. The indirect gap of 3.59 eV of SrS is in good agreement with theoretical calculations (Bhattacharjee and Chattopadhyaya 2017a, b; Debnath et al. 2018) found with TB–mBJ, and it is better than that of the values of Refs. Bhattacharjee and Chattopadhyaya (2017a, b), Debnath et al. (2018) obtained by the GGA–WC (Wu and Cohen 2006) and the generalized gradient approximation of Perdew–Burke–Ernzerhof (GGA–PBE) (Perdew et al. 1996) because the TB–mBJ potential is suitable to improve the gaps of band structures with respect to the local density approximation and all forms of the generalized gradient approximation functional (Bhattacharjee and Chattopadhyaya 2017a, b; Tran and Blaha 2009; Chattopadhyaya and Bhattacharjee 2017). The Fig. 2 revealed that the majority spins are metallic because some bands dominate the Fermi level (E_F), while a gap arises around E_F for minority spins. Consequently, the $\text{Sr}_{0.875}\text{Ti}_{0.125}\text{S}$ compound is a half-metallic ferromagnetic with a spin polarization of 100%. The minority spin bands show that $\text{Sr}_{0.875}\text{Ti}_{0.125}\text{S}$ compound has a direct HMF gap of 2.844 eV situated at Γ high symmetry point between the VBM and CBM. In addition, the half-metallic gap is defined as the minimum energy gap of a spin excitation with respect to the Fermi level required to create a hole in the valence band maximum or to generate an electron in the

Table 2 Computed indirect band gap ($E^{\Gamma X}$) for SrS, half-metallic ferromagnetic gap (G_{HMF}) and half-metallic gap (G_{HM}) of minority-spin bands for $\text{Sr}_{0.875}\text{Ti}_{0.125}\text{S}$

Compound	G_{HMF} (eV)	G_{HM} (eV)	$E^{\Gamma X}$ (eV)	Method
This work				
SrS			3.62	TB–mBJ
$\text{Sr}_{0.875}\text{Ti}_{0.125}\text{S}$	2.844	1.245		TB–mBJ
Other calculations				
SrS			2.303 ^a , 2.305 ^b	GGA–WC
			2.3 ^c	GGA–PBE
			3.798 ^a , 3.686 ^b	TB–mBJ
			3.798 ^c	
		4.32 ^d		Experimental

^aBhattacharjee and Chattopadhyaya (2017a)

^bDebnath et al. (2018)

^cBhattacharjee and Chattopadhyaya (2017b)

^dKaneko and Koda (1988)

conduction band minimum (Yao et al. 2005). In $\text{Sr}_{0.875}\text{Ti}_{0.125}\text{S}$ minority-spin bands, the minimum energy gap for a spin excitation is located between the conduction band minimum and the Fermi level. Thus, the half-metallic gap of 1.245 eV describes the minimal energy gap of a spin excitation to generate an electron in the conduction band minimum (Doumi et al. 2015a).

The Fig. 3 shows the contribution of partial and total densities of states (DOS) of majority-spin and minority-spin states of $\text{Sr}_{0.875}\text{Ti}_{0.125}\text{S}$ with respect to the Fermi level (E_F). In the $\text{Sr}_{0.875}\text{Ti}_{0.125}\text{S}$ supercell, the Ti atom is situated in the crystal field originated from the octahedral environment of S ions, leading to split of 3d-Ti states into two levels such as the three low-lying t_{2g} (d_{xy} , d_{xz} , and d_{yz}) states and two high-lying e_g (d_{z^2} and $d_{x^2-y^2}$) states (Doumi et al. 2015a, d). From the partial DOS of 3d-Ti states, we have depicted that the t_{2g} are lower than that e_g states, confirming that Ti atom is positioned in the octahedral surrounding. The densities of states of two spin directions of $\text{Sr}_{0.875}\text{Ti}_{0.125}\text{S}$ are symmetric in the range of -4.2 to -1.6 eV of valence bands, which are originated from the main contributions of p states of S atom and by the small contributions of the 3d-Ti and p-Sr states. Also, the DOS of the two spin channels are mainly dominated by the 3d-Ti states in the range of 1.3 to 4 eV of bottom of conduction bands. From the total DOS, we can clearly see that the density of states are metallic for majority spins and they have a band gap for minority spins, leading to a half-metallic behavior for $\text{Sr}_{0.875}\text{Ti}_{0.125}\text{S}$ compound with a spin polarization of 100%.

Fig. 3 Spin-polarized total and partial densities of states (DOS) of $\text{Sr}_{0.875}\text{Ti}_{0.125}\text{S}$. (Fermi level (E_F) is set to zero)

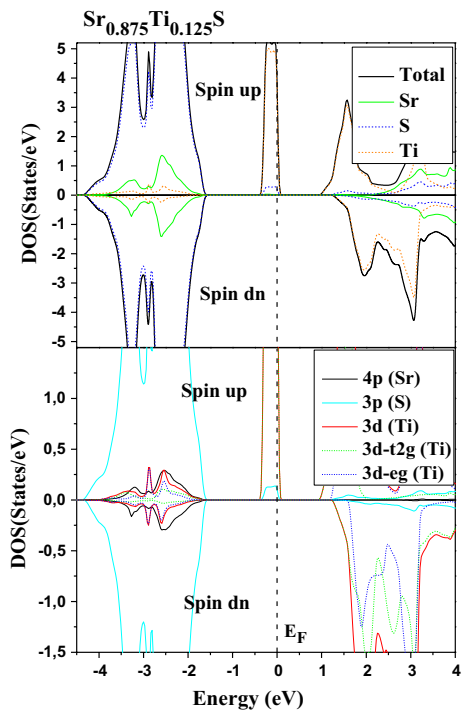


Table 3 Computed total and partial magnetic moments of Ti, Sr and S atoms and in the interstitial site (in Bohr magneton μ_B) for $\text{Sr}_{0.875}\text{Ti}_{0.125}\text{S}$

Compound	Total (μ_B)	Ti (μ_B)	Sr (μ_B)	S (μ_B)	Interstitial (μ_B)
$\text{Sr}_{0.875}\text{Ti}_{0.125}\text{S}$	2	1.656	0.003	0.008	0.334

3.3 Magnetic moments

In the $\text{Sr}_{0.875}\text{Ti}_{0.125}\text{S}$ compound, the Ti atom is substituted at the Sr site, which contributes two electrons to S atoms. Therefore, the 3d states of Ti ion become partially occupied with two electrons, which generate a total magnetic moment of 2 μ_B (μ_B is the Bohr magneton). This value of total magnetic moment is mainly formed by the partial magnetic moment of Ti atom and minor local magnetic moments are induced in the non magnetic Sr and S sites due to the strong p-d exchange interaction between the p-S and 3d-Ti levels. The crystal field of surrounding S ions split d-Ti states into t_{2g} and e_g states, which create bonding and anti-bonding states. For minority-spin states, a large p-d exchange interaction is responsible for the separation of bonding and anti-bonding states owing to the strong p-d hybridization between p-S and d-Ti states. This mechanism is responsible for attribution of different electrons densities in Sr, S and Ti atoms of $\text{Sr}_{0.875}\text{Ti}_{0.125}\text{S}$ compound, and hence the ferromagnetism emerges in this system (Saini et al. 2012).

Comparing to our result of total magnetic moment of 2 μ_B of $\text{Sr}_{0.875}\text{Ti}_{0.125}\text{S}$, the calculations of $\text{Sr}_{0.875}\text{V}_{0.125}\text{S}$ (Doumi et al. 2015a) and $\text{Sr}_{0.875}\text{Cr}_{0.125}\text{S}$ (Doumi et al. 2015d) show total magnetic moments of 3 and 4 μ_B arising from the partially occupied d-V and d-Cr states, respectively. The d states are partially filled by three electrons for V and four electrons for Cr because the V and Cr ions have one and two extra electrons than Ti. Consequently, the unpaired electrons of d states such as two for Ti, three for V and four for Cr ions generate total magnetic moments of 2, 3 and 4 μ_B for $\text{Sr}_{0.875}\text{Ti}_{0.125}\text{S}$, $\text{Sr}_{0.875}\text{V}_{0.125}\text{S}$ and $\text{Sr}_{0.875}\text{Cr}_{0.125}\text{S}$ compounds, respectively.

The partial and total magnetic moments of relevant atoms and in the interstitial site of $\text{Sr}_{0.875}\text{Ti}_{0.125}\text{S}$ material are given in Table 3. The positive magnetic moments of Ti, Sr and S atoms describe the ferromagnetic interaction between the magnetic spins of these atoms. In conclusion, the results of magnetic moments confirm the ferromagnetic feature of $\text{Sr}_{0.875}\text{Ti}_{0.125}\text{S}$ compound.

4 Conclusion

The structural, electronic and ferromagnetic properties of SrS and $\text{Sr}_{0.875}\text{Ti}_{0.125}\text{S}$ compound were investigated by employing the first-principle calculations of density functional theory. The results of structural parameters with GGA-WC and band gap with TB-mBJ of SrS are in good agreement with other theoretical calculations using the same exchange potentials. The lattice parameter of $\text{Sr}_{0.875}\text{Ti}_{0.125}\text{S}$ is lower than that of SrS owing to the difference between Sr and Ti ionic radii. The electronic structures of $\text{Sr}_{0.875}\text{Ti}_{0.125}\text{S}$ exhibit a half-metallic ferromagnetic behavior with a half-metallic gap of 1.245 and spin polarization of 100%. The ferromagnetic nature of $\text{Sr}_{0.875}\text{Ti}_{0.125}\text{S}$ is confirmed by the ferromagnetic interaction between magnetic moments of Ti, Sr and S atoms. The integral total magnetic

moment of $2 \mu_B$ and the wide half-metallic gap suggest that the $\text{Sr}_{0.875}\text{Ti}_{0.125}\text{S}$ is a right half-metal. Therefore, the $\text{Sr}_{0.875}\text{Ti}_{0.125}\text{S}$ is promising material for possible spin-injection applications in semiconductor spintronics.

References

- Addadi, Z., Doumi, B., Mokaddem, A., Elkeurti, M., Sayede, A., Tadjer, A., Dahmane, F.: Electronic and ferromagnetic properties of 3d (V)-doped (BaS) barium sulfide. *J. Supercond. Novel Magn.* **30**(4), 917–923 (2017)
- Becke, A.D., Johnson, E.R.: A simple effective potential for exchange. In: AIP (2006)
- Berriah, K., Doumi, B., Mokaddem, A., Elkeurti, M., Sayede, A., Tadjer, A., Araújo, J.P.: Theoretical investigation of electronic performance, half-metallicity, and magnetic properties of Cr-substituted BaTe. *J. Comput. Electron.* **17**(3), 909–919 (2018)
- Bhattacharjee, R., Chattopadhyaya, S.: Effects of barium (Ba) doping on structural, electronic and optical properties of binary strontium chalcogenide semiconductor compounds—a theoretical investigation using DFT based FP-LAPW approach. *Mater. Chem. Phys.* **199**, 295–312 (2017a)
- Bhattacharjee, R., Chattopadhyaya, S.: Effects of doping of calcium atom (s) on structural, electronic and optical properties of binary strontium chalcogenides—a theoretical investigation using DFT based FP-LAPW methodology. *Solid State Sci.* **71**, 92–110 (2017b)
- Blaha, P., Schwarz, K., Madsen, G.K.H., Kvasnicka, D., Luitz, J.: WIEN2K: an augmented plane wave and local orbitals program for calculating crystal properties. In: Vienna, K. (ed.) University of Technology, Schwarz, Austria (2001)
- Chattopadhyaya, S., Bhattacharjee, R.: Theoretical study of structural, electronic and optical properties of BaxPb1-xS , BaxPb1-xSe and BaxPb1-xTe ternary alloys using FP-LAPW approach. *J. Alloy. Compd.* **694**, 1348–1364 (2017)
- Cherfi, Y., Mokaddem, A., Bensaid, D., Doumi, B., Sayede, A., Dahmane, F., Tadjer, A.: A novel theoretical investigation of electronic structure and half-metallic ferromagnetism in 3d (V)-doped InP for spintronic applications. *J. Supercond. Novel Magn.* **29**(7), 1813–1819 (2016)
- Cui, Y., Zhu, J., Tao, H., Liu, S., Lv, Y., He, M., Song, B., Chen, Y., Zhang, Z.: Magnetic properties of diluted magnetic semiconductors Li (Zn, TM) N with decoupled charge and spin doping (TM: V, Cr, Mn, Fe, Co and Ni). *Comput. Mater. Sci.* **158**, 260–264 (2019)
- Dadsetani, M., Pourghazi, A.: Optical properties of strontium monochalcogenides from first principles. *Physical Review B* **73**(19), 195102 (2006)
- Debnath, B., Sarkar, U., Debbarma, M., Bhattacharjee, R., Chattopadhyaya, S.: Tuning of electronic band gaps and optoelectronic properties of binary strontium chalcogenides by means of doping of magnesium atom (s)-a first principles based theoretical initiative with mBJ, B3LYP and WC-GGA functionals. *Phys. B* **530**, 53–68 (2018)
- Dietl, T., Ohno, H., Matsukura, F., Cibert, J., Ferrand, E.D.: Zener model description of ferromagnetism in zinc-blende magnetic semiconductors. *Science* **287**(5455), 1019–1022 (2000)
- Doumi, B., Mokaddem, A., Dahmane, F., Sayede, A., Tadjer, A.: A novel theoretical design of electronic structure and half-metallic ferromagnetism in the 3d (V)-doped rock-salts SrS , SrSe , and SrTe for spintronics. *RSC Adv.* **5**(112), 92328–92334 (2015a)
- Doumi, B., Mokaddem, A., Sayede, A., Boutaleb, M., Tadjer, A., Dahmane, F.: Half-metallic ferromagnetic property related to spintronic applications in 3d (V, Cr, and Mn)-doped GaP DMSs. *J. Supercond. Novel Magn.* **28**(10), 3163–3172 (2015b)
- Doumi, B., Mokaddem, A., Sayede, A., Dahmane, F., Mogulkoc, Y., Tadjer, A.: First-principles investigations on ferromagnetic behaviour of Be1-xVxZ ($Z=\text{S, Se and Te}$) ($x=0.25$). *Superlattices Microstruct.* **88**, 139–149 (2015c)
- Doumi, B., Mokaddem, A., Temimi, L., Beldjoudi, N., Elkeurti, M., Dahmane, F., Sayede, A., Tadjer, A., Ishak-Boushaki, M.: First-principle investigation of half-metallic ferromagnetism in octahedrally bonded Cr-doped rock-salt SrS , SrSe , and SrTe . *Eur. Phys. J. B* **88**(4), 93 (2015d)
- Emam-Ismail, M., El-Hagary, M., Shaaban, E., Moustafa, S., Gad, G.: Spectroscopic ellipsometry and morphological characterizations of nanocrystalline Hg1-xMnxO oxide diluted magnetic semiconductor thin films. *Ceram. Int.* **45**(7), 8380–8387 (2019)
- Ghosh, B., Bagani, K., Majumder, S., Modak, M., Ray, M., Sardar, M., Banerjee, S.: Can one introduce long range ferromagnetism by doping transition metal in wide band gap semiconducting ZnO? *Results Phys.* **12**, 623–628 (2019a)

- Ghosh, S., Choubey, C., Sil, A.: Photocatalytic response of Fe Co, Ni doped ZnO based diluted magnetic semiconductors for spintronics applications. *Superlattices Microstruct.* **125**, 271–280 (2019b)
- Hohenberg, P., Kohn, W.: Inhomogeneous electron gas. *Phys. Rev.* **136(3B)**, B864–871 (1964)
- Kaneko, Y., Koda, T.: New developments in IIa–VIb (alkaline-earth chalcogenide) binary semiconductors. *J. Cryst. Growth* **86(1–4)**, 72–78 (1988)
- Kohn, W., Sham, L.J.: Self-consistent equations including exchange and correlation effects. *Phys. Rev.* **140(4A)**, A1133 (1965)
- Lakhdari, H., Doumi, B., Mokaddem, A., Sayede, A., Araújo, J.P., Tadjer, A., Elkeurti, M.: Investigation of the substituting effect of chromium on the electronic structures and the half-metallic ferromagnetic properties of BaO. *J. Supercond. Novel Magn.* **32(6)**, 1781–1790 (2019)
- Lei, G., Liu, X.-X., Xie, H.-H., Li, L., Gao, Q., Deng, J.-B.: First-principle study of half-metallic ferromagnetism in rocksalt XO (X=Li, K, Rb, Cs). *J. Magn. Magn. Mater.* **397**, 176–180 (2016)
- Lin, H.-F., Lau, W.-M., Zhao, J.: Magnetism in the p-type Monolayer II-VI semiconductors SrS and SrSe. *Sci. Rep.* **7**, 45869 (2017)
- Linneweber, T., Binemann, J., Löw, U., Gebhard, F., Anders, F.: Exchange couplings for Mn ions in CdTe: validity of spin models for dilute magnetic II–VI semiconductors. *Phys. Rev. B* **95(4)**, 045134 (2017)
- Miyagawa, H., Funaki, N., Koshihara, S., Takahashi, N., Inada, Y., Mizumaki, M., Kawamura, N., Suzuki, M.: Origin of magnetization in diluted magnetic semiconductor GaGdAs monolayer and superlattice. *J. Magn. Magn. Mater.* **476**, 213–217 (2019)
- Monkhorst, H.J., Pack, J.D.: Special points for Brillouin-zone integrations. *Phys. Rev. B* **13(12)**, 5188–5192 (1976)
- Murnaghan, F.: The compressibility of media under extreme pressures. *Proc. Natl. Acad. Sci. U.S.A.* **30(9)**, 244–247 (1944)
- Pack, J.D., Monkhorst, H.J.: “Special points for Brillouin-zone integrations”—a reply. *Phys. Rev. B* **16(4)**, 1748–1749 (1977)
- Pandey, R., Sivaraman, S.: Spectroscopic properties of defects in alkaline-earth sulfides. *J. Phys. Chem. Solids* **52(1)**, 211–225 (1991)
- Perdew, J.P., Burke, K., Ernzerhof, M.: Generalized gradient approximation made simple. *Phys. Rev. Lett.* **77(18)**, 3865–3868 (1996)
- Ruoff, A., Grzybowski, T.: *Solid State Physics Under Pressure*, edited by S. Minomura (Terra Scientific, Tokyo) (1985)
- Saini, H.S., Singh, M., Reshak, A.H., Kashyap, M.K.: Emergence of half metallicity in Cr-doped GaP dilute magnetic semiconductor compound within solubility limit. *J. Alloy. Compd.* **536**, 214–218 (2012)
- Sajjad, M., Manzoor, S., Zhang, H., Noor, N., Alay-e-Abbas, S., Shaukat, A., Khenata, R.: The half-metallic ferromagnetism character in Be1–xVxY (Y=Se and Te) alloys: An ab initio study. *J. Magn. Magn. Mater.* **379**, 63–73 (2015)
- Salam, M.M.A.: First principles study of structural, elastic and electronic structural properties of strontium chalcogenides. *Chin. J. Phys.* **57**, 418–434 (2019)
- Sato, K., Katayama-Yoshida, H.: Material design of GaN-based ferromagnetic diluted magnetic semiconductors. *Jpn. J. Appl. Phys.* **40(5B)**, L485–L487 (2001)
- Shahjahan, M., Nizu, S.Y.: Numerical study of magnetic states and magnetic properties of transition metal doped II-VI oxide semiconductors. *Comput. Condens. Matter* **16**, e00305 (2018)
- Singh, D.J., Nordstrom, L.: *Planewaves, Pseudopotentials, and the LAPW method*. Springer Science & Business Media, (2006)
- Syassen, K.: Pressure-induced structural transition in SrS. *Physica Status Solidi* **91(1)**, 11–15 (1985)
- Torquato, R., Shirsath, S., Kiminami, R., Costa, A.: Synthesis and structural, magnetic characterization of nanocrystalline Zn1-xCoxO diluted magnetic semiconductors (DMS) synthesized by combustion reaction. *Ceram. Int.* **44(4)**, 4126–4131 (2018)
- Tran, F., Blaha, P.: Accurate band gaps of semiconductors and insulators with a semilocal exchange-correlation potential. *Phys. Rev. Lett.* **102(22)**, 226401 (2009)
- Varshney, D., Kaurav, N., Kinge, R., Singh, R.: High pressure structural (B1–B2) phase transition and elastic properties of II–VI semiconducting Sr chalcogens. *Comput. Mater. Sci.* **41(4)**, 529–537 (2008)
- Wang, M., Marshall, R., Edmonds, K., Rushforth, A., Campion, R., Gallagher, B.: Determining Curie temperatures in dilute ferromagnetic semiconductors: high Curie temperature (Ga, Mn) As. *Appl. Phys. Lett.* **104(13)**, 132406 (2014)
- Wu, Z., Cohen, R.E.: More accurate generalized gradient approximation for solids. *Phys. Rev. B* **73(23)**, 235116 (2006)
- Wu, S.Y., Liu, H., Gu, L., Singh, R., Budd, L., Van Schilfgaarde, M., McCartney, M., Smith, D.J., Newman, N.: Synthesis, characterization, and modeling of high quality ferromagnetic Cr-doped AlN thin films. *Appl. Phys. Lett.* **82(18)**, 3047–3049 (2003)

- Yamashita, N., Ohira, T., Mizuochi, H., Asano, S.: Luminescence of Pb²⁺-centers in SrS and SrSe phosphors. *J. Phys. Soc. Jpn.* **53**(1), 419–426 (1984)
- Yang, X., Wang, Y., Yan, H., Chen, Y.: Effects of epitaxial strains on spontaneous polarizations and band gaps of alkaline-earth-metal oxides MO (M=Mg, Ca, Sr, Ba). *Comput. Mater. Sci.* **121**, 61–66 (2016)
- Yao, K., Gao, G., Liu, Z., Zhu, L.: Half-metallic ferromagnetism of zinc-blende CrS and CrP: a first-principles pseudopotential study. *Solid State Commun.* **133**(5), 301–304 (2005)
- Yunusov, Z., Yuldashev, S.U., Kwon, Y., Kim, D., Lee, S., Jeon, H., Jung, H., Kim, A., Kang, T.: Band gap engineering of ZnMnO diluted magnetic semiconductor by alloying with ZnS. *J. Magn. Magn. Mater.* **446**, 206–209 (2018)